Developmental Biology **253,** 66–83 (2003)
doi:10.1006/dbio.2002.0865

The Step-Wise Assembly of a Functional Nucleolus in Preimplantation Mouse Embryos Involves the Cajal (Coiled) Body

Olga Zatsepina,*,† Christine Baly,†,[1] Martine Chebrout,† and Pascale Debey†,[2]

**A. N. Belozersky Institute of Physico-Chemical Biology, Moscow State University, 119992, Moscow, Russia; and †INRA UC 806/EA 2703 MNHN, IFR 63, Institut de Biologie Physico-Chimique, 13 rue P. et M. Curie, F75005, Paris, France*

After fertilization, ribosomal RNA synthesis is silenced during a period which depends on the species. Data concerning the reassembly of a functional nucleolus remain scarce. We have examined by immunocytochemistry, Western blots, and BrUTP microinjection the dynamics of major nucleolar proteins during the first cycles of mouse embryogenesis, in relation to rDNA transcription sites and coilin, a marker of Cajal bodies. We show that: (1) the reinitiation of rDNA transcription occurs at the two-cell stage, 44–45 h after hCG injection (hphCG), at the surface of the nucleolar precursor bodies (NPBs), where the RNA polymerase I (pol I) transcription complex is recruited 4–5 h before; (2) the NPBs are not equal in their ability to support recruitment of pol I and rDNA transcription; (3) maternally inherited fibrillarin undergoes a dynamic redistribution during the second cell stage, together with coilin, leading to the assembly of the Cajal body around 40 hphCG; and (4) the pol I complex is first recruited to the Cajal body before reaching its rDNA template. We also find that fibrillarin and B23 are both directly assembled around NPBs prior to ongoing pre-rRNA synthesis. Altogether, our results reveal a role of the Cajal bodies in the building of a functional nucleolus.

Key Words: **Cajal body; development; mouse preimplantation embryos; nucleologenesis; nucleolus precursor body; polymerase I.**

INTRODUCTION

The nucleolus is a complex nuclear territory where ribosomal RNAs (rRNAs) are synthesized and processed and preribosomal particles are assembled (for review, see Shaw and Jordan, 1995; Scheer and Hock, 1999). At the ultrastructural level, the functional nucleolus is composed of three well defined subcompartments, namely the fibrillar center (FC), the dense fibrillar component (DFC), and the granular component (GC) (Hadjiolov, 1985; Derenzini *et al.*, 1990). The assignment of a given step of rRNA synthesis and maturation to any one of these compartments has been the subject of intense studies: the rDNAs, RNA polymerase I (pol I) and its associated factors, the upstream binding factor (UBF) and the promoter selectivity factor (SL1), were found in FCs, in the DFC, or in both compartments (Scheer and Rose, 1984; Zatsepina *et al.*, 1993; Biggiogera *et al.*, 2001). The pre-rRNA processing machinery, composed mainly of small nucleolar RNAs (snoRNAs) and proteins such as nucleolin, fibrillarin, and B23/nucleophosmin, were found in the DFC and GC (Spector *et al.*, 1984; Shaw and Jordan, 1995; Azum-Gelade *et al.*, 1994; Cmarko *et al.*, 2000). Nascent pre-rRNA transcripts are mainly located in the FC and/or the inner part of the DFC (Ochs *et al.*, 1985b; Thiry and Goessens, 1991; Dundr and Raska, 1993; Cmarko *et al.*, 2000, Thiry *et al.*, 2000).

[1] Present address: BCM, INRA, Domaine de Vilvert, 78352 Jouy-en-Josas Cedex, France.

[2] To whom correspondence should be addressed. Fax: +00 33 (0)1 58 41 50 20. E-mail: debey @ibpc.fr.

Abbreviations: CB, Cajal body; DFC, dense fibrillar component; FC, fibrillar center; GC, granular component; GV, germinal vesicle; hCG, human chorionic Gonadotropin; hnRNA, heterogenous nuclear RNA; NDF, nucleolus-derived foci; NLB, nucleolus-like body; NOR, nucleolar organizing region; NPB, nucleolus-precursor body; pCB, pre-coiled (Cajal) body; PNB, prenucleolar body; pol I, RNA polymerase I; snRNA, small nuclear RNAs; snoRNA, small nucleolar RNA; UBF, upstream binding factor.

0012-1606/03 $35.00

When cells enter mitosis, rRNA synthesis is switched down, the nucleolar compartment disappears, and its structural components are mainly disassembled. Major molecular constituents of the rDNA transcription machinery, such as pol I, UBF, and SL1, remain attached to the rDNA arrays forming the nucleolar-organizing regions (NORs) (Scheer and Rose, 1984; Roussel *et al.,* 1996; Gebrane-Younes *et al.,* 1997), whereas pre-rRNA processing components are relocated around the chromosomes and dispersed in the cytoplasm and in particles termed nucelolus-derived foci (NDF) (Gautier *et al.,* 1992; Azum-Gelade *et al.,* 1994; Dundr *et al.,* 1997). The nucleolus is gradually reassembled at telophase, upon resumption of rDNA transcription that is apparently controlled by alterations in the phosphorylation status of the pol I transcription factors (Voit *et al.,* 1999). Various types of prenucleolar bodies (PNBs) are formed, which contain snoRNAs, different sets of pre-rRNA maturation factors, and pre-rRNA sequences (Ochs *et al.,* 1985a; Jimenez-Garcia *et al.,* 1994; Fomproix and Hernandez-Verdun, 1999; Dundr *et al.,* 2000). The postmitotic reformation of the nucleolus involves both transcription-independent recruitment of processing factors and pre-rRNAs to the NOR-associated transcription machinery (Dousset *et al.,* 2000) and transcription-dependent fusion of prenucleolar bodies with the NORs (Ochs *et al.,* 1985a; Jimenez-Garcia *et al.,* 1994; Fomproix *et al.,* 1998).

In contrast to somatic cells, early development is characterized by a period where both pol II- and pol I-dependent transcription remain switched off during a number of cell cycles that depend on the species (for review, see Latham, 1999). Usually, pol II activity is restored before that of pol I. In mice, incorporation of BrUTP (Bouniol *et al.,* 1995) and expression of reporter genes (Thompson *et al.,* 1995) show that pol II transcription is reinitiated at the end of the first cell cycle. The data on the onset of pol I transcription are more uncertain, as newly synthesized rRNA was observed as soon as the end of the two-cell (Knowland and Graham, 1972; Clegg and Piko, 1983, Engel *et al.,* 1977) or only at the 4-cell stage (Geuskens and Alexandre, 1984).

During this period, the characteristic nucleolus is not present, but so-called nucleolar-precursor bodies (NPBs) are formed. Morphologically, NPBs are profoundly different from the postmitotic PNBs, NDF, or transcribing nucleoli found in somatic cells, and are reminiscent of the nucleolus-like bodies (NLBs) formed in mature germinal vesicle (GV) oocytes before ovulation. In mouse, rat, pig, rabbit, and humans, NLBs and NPBs are characterized by disappearance of the tripartite organization that is reduced to a fully compact fibrillar mass lacking FCs and the DFC (Fakan and Odartchenko, 1980; Takeuchi and Takeuchi, 1986; for review, see Flechon and Kopecny, 1998 and references therein). It was shown by different approaches that NPBs do not contain DNA, but mainly RNA, U3-type RNPs, nucleolar (fibrillarin, nucleolin, B23), and ribosomal proteins, as well as nonnucleolar spliceosomal factors, such as hnRNPs and snRNPs (Fakan and Odartchenko, 1980; Prather *et al.,* 1990; Kopecny *et al.,* 1995, 1996; Biggiogera *et al.,* 1990, 1994).

Despite a number of immunocytochemical studies on the behavior of the nucleolar proteins in early mouse embryos (e.g., Baran *et al.,* 1995, 2001; Cuadros-Fernandez and Esponda, 1996; Ferreira and Carmo-Fonseca, 1995), the dynamics of their appearance and of the reassembly of the rDNA transcription machinery, as well as the implication of NPBs in the formation of mature nucleoli, still remain unclear. Also, data on the role of zygotic transcription and translation in the pol I complex formation are lacking. We showed previously that, in mouse GV oocytes, the majors proteins of rRNA synthesis and maturation machinery, such as UBF, RPA116, RPA/PAF53, and fibrillarin, remain present and located at the periphery of the NLBs even when the pol I transcriptional activity has ceased (Zatsepina *et al.,* 2000). We also showed that, contrary to what happens during mitosis, UBF and pol I dissociate from the chromosomes and are apparently degraded during the subsequent meiotic divisions. This indicates that, in fertilized embryos, the reformation of the nucleolus is not nucleated by the pol I transcription complex carried by maternal chromosomes, but requires its *de novo* assembly.

Initially described as "nucleolar accessory bodies" by Ramon y Cajal, "coiled bodies" recently renamed "Cajal bodies" (CBs), are highly dynamic nuclear structures functionally linked to the nucleolus (for review, see Gall, 2000). Besides their specific marker, the phosphoprotein p80-coilin (Raska *et al.,* 1991), CBs contain also other typical nucleolar proteins, such as fibrillarin, Nopp140, and the ribosomal protein S6 (Raska *et al.,* 1991; Isaac *et al.,* 1998). Transient expression of some coilin mutants results in the disruption of the nucleolar architecture and loss of pol I activity (Bohmann *et al.,* 1995), whereas treatment of cells with the serine/threonine kinase inhibitor okadaic acid leads to the accumulation of coilin within the nucleoli (Lyon *et al.,* 1997; Sleeman *et al.,* 1998). CBs also contain snRNPs and snoRNPs (Carmo-Fonseca *et al.,* 1992; Jimenez-Garcia *et al.,* 1994; Narayanan *et al.,* 1999) and seem to be involved in their transport and maturation (Sleeman and Lamond, 1999; Narayanan *et al.,* 1999**)**. In mouse embryos, Ferreira and Carmo-Fonseca (1995) described two types of CB-related structures: precoiled bodies (pCBs) and the true CBs. Both structures were assembled in the maternal and paternal pronuclei of one-cell embryos, contained coilin, fibrillarin, and splicing snRNPs, but differed in ultrastructure and size.

The goal of the present study was to analyze in detail the dynamics of reactivation of ribosomal genes and assembly of a functional nucleolus in early mouse embryos. Using indirect immunofluorescent detection of proteins and BrUTP-labeled nascent rRNA transcripts as well as Western blots, we show that pol I-dependent transcription is activated in the second part of the two-cell cycle (around 45 h after hCG) and the pol I machinery starts to assemble 4–5 h before the rDNA transcription onset, mainly upon *de novo* protein synthesis. We show also that components of the pol

I transcription machinery are first recruited to CB, before associating with rDNA, which suggests that this nuclear compartment plays a role in the nucleologenesis. Finally, we provide evidence that, at the two- and beginning of the four-cell stages, the population of NPBs is heterogeneous, with only some of them bearing the active rDNA transcription and rRNA processing machineries.

MATERIALS AND METHODS

Recovery of Oocytes or Embryos

Five-to eight-week-old C57×CBA female mice were superovulated by intraperitoneal injection of 5 IU of pregnant mare serum gonadotropin (PMSG; Intervet, Angers, France) followed 46–52 h later by 5 IU of human chorionic gonadotropin (hCG; Intervet). They were sacrificed, and embryos were collected at different times after hCG injection (hphCG) directly from ampullae (one-cell stage) or oviducts (two- to eight-cell stages) and kept in M2 medium (Bouniol-Baly *et al.*, 1999) at 37°C before use. All experiments were performed on *in vivo* developed embryos, except in the case of drug treatments, where *in vitro* culture was necessary. *In vitro* culture was performed in small drops of Whitten's medium (Bouniol-Baly *et al.*, 1999) covered by paraffin oil (BdH Laboratory Supplies, Poole, UK) at 37°C in a 5% CO_2 atm.

Fully grown GV oocytes were obtained from hyperstimulated females (PMSG- injected) by random puncture of the ovaries. They were freed from follicular cells by gentle pipetting, and kept at 37°C in M2 medium containing 100 μg/ml of dibutiryl cAMP (dbcAMP; Sigma, St. Louis, MO) to avoid meiotic maturation.

To obtain *in vivo* matured MII oocytes, stimulated 4- to 6-week-old females were sacrificed 14–17 hphCG and MII oocytes were collected from ampullae, released from cumulus cells with 1 mg/ml hyaluronidase for 2 min, and used immediately.

Parthenogenetic activation of ovulated MII oocytes was performed at 16–17 hphCG by incubation in 8% ethanol for 6 min (Borsuk *et al.*, 1996) or in 10 μg/ml cycloheximide for 30 min. After thorough rinsing in M2 medium, activated oocytes were further cultured in Whitten's medium as described above for the fertilized embryos.

Assessment of rRNA Synthesis

Ribosomal RNA synthesis was monitored following Bouniol-Baly *et al.* (1999) by cytoplasmic microinjection of 1 ± 0.5 pl of a solution containing 100 mM BrUTP (Sigma), 50 μg/ml α-amanitin (Sigma), 140 mM KCl, and 2 mM Pipes, pH 7.4. Embryos were then recovered in Whitten's medium containing α-amanitin (10 μg/ml) for 10–30 min, rinsed, and fixed for immunolabeling. Embryos not treated with α-amanitin were included in each experiment as controls of the proper BrUTP incorporation and detection.

Drug Treatments

When necessary, isolated embryos were cultured in Whitten's medium containing either 0.25 μM actinomycin D, a potent pol I inhibitor, or 50 μg/ml of the protein synthesis inhibitor, cycloheximide. Treated embryos were fixed at various times following the addition of the drug. All drugs were purchased from Sigma.

Antibodies and Immunolabeling

Embryos were fixed with 2% paraformaldehyde (PFA) for 1 h at room temperature, followed by permeabilization with 0.2% Triton X-100 in PBS for 1 h at room temperature. Alternatively, they were simultaneously fixed and permeabilized by incubation in HPEM buffer (60 mM Pipes, 25 mM Hepes, 10 mM EGTA, 2 mM $MgCl_2$, pH 6.9) containing 1% PFA and 0.2% Triton X-100 for 40 min at room temperature. They were then blocked in 2% BSA in PBS and processed for *in toto* single or double immunolabeling (see below).

The following primary antibodies were used (dilutions were in PBS supplemented with 2% BSA): human anti-UBF serum (Zatsepina *et al.*, 1993, 2000; dilution 1:100); mouse polyclonal serum against a 116-kDa subunit of RNA pol I, RPA116 (a gift from Dr. I. Grummt, German Cancer Research Center, Heidelberg, Germany; dilution 1:70); human autoimmune serum against fibrillarin (Magoulas *et al.*, 1998; dilution 1:200); mouse monoclonal antibody (mAb) to fibrillarin (a gift from Dr. R. Ochs, W. M. Kerk Autoimmune Disease Center, La Jolla, CA; Ochs and Press, 1992; dilution 1:100); mouse mAb to B23/nucleophosmin (Zatsepina *et al.*, 1997; a gift from Dr. P. K. Chan, Baylor College of Medicine, Houston, TX; dilution 1:50); mouse mAb against BrdU that also recognizes BrU (Boehringer, Mannheim, Germany; dilution 1:50); rabbit polyclonal anti-coilin antibody (kindly provided by Dr. A. Lamond University of Dundee, Dundee, UK, dilution 1:400); and anti-Sm mouse mAb Y12 (a gift from Dr. J. A. Steiz, Yale University, New Haven, CT; dilution 1:800). Whole embryos were incubated with primary antibodies taken in appropriate combinations, for 1 h at room temperature or overnight at 4°C, washed in PBS containing 2% BSA for 1 h, and incubated with appropriate combinations of the secondary antibodies for 1 h at room temperature. As secondary antibodies, FITC-conjugated anti-human IgG(H+L) (Jackson Immunoresearch Laboratories, West Grove; dilution 1:100); rhodamin-conjugated or FITC-conjugated anti-mouse IgG(H+L); (Jackson Immunoresearch Laboratories; dilution 1:100); Texas-Red- or FITC-conjugated anti-rabbit IgG(H+L) (Jackson Immunoresearch Laboratories, dilution 1:100) were used. Specimens were stained with 2 μg/ml Hoechst 33242 for 15 min and thoroughly washed with PBS. For analysis by conventional fluorescence microscopy, embryos or activated oocytes were placed on microscope slides, and excess PBS was carefully removed and replaced by Citifluor (Citifluor Products, Canterbury, UK). Coverslips were then fixed with paraffin. In order to avoid flattening of embryos in the case of confocal microscopy, a spacer between the slide and the coverslip was introduced.

For immunofluorescence controls, PBS was used instead of the primary antibodies. The specificity of BrUTP incorporation in newly synthesized rRNA was monitored by incubating embryos with 0.2–0.5 μg/ml actinomycin D for 1–3 h before BrUTP microinjection. This treatment abolished BrUTP incorporation completely.

Fluorescence Microscopy and Image Analysis

Conventional fluorescence microscopy was performed on an Axiovert inverted microscope (Carl Zeiss, Oberkochen, Germany) by using a filter wheel for the excitation light, a triple-band dichroic mirror and filter set for emitted light, and a 100× Plan Neofluar objective (NA 1.3). Images were captured by a cooled CCD camera (Photometrics, Tucson, AZ; type KAF 1400, 12 bits of dynamic range) and processed through the IPLab Spectrum software (Vysis, France). With this setup, images taken at two different wavelengths were absolutely coincident. In addition, we checked

in each experiment to make sure that there was no overlap between rhodamin and fluorescein signals using this combination of filters.

Confocal microscopy was performed on an inverted Nikon (Nikon France, Paris) microscope equipped with the Bio-Rad Laser-Sharp MRC-1024 confocal laser scanning software (Elexience, Paris, France). The objective was a Nikon Fluor oil-immersion 100× (NA 1.3), and the pinhole was set up between 1.5 and 2.8 μm. The 488- and 568-nm wavelengths of the laser were used for excitation of fluorescein or rhodamin and Texas Red fluorescence, respectively.

Western Blots

A total of 190–200 oocytes at either GV or MII stages and 200–350 embryos at either one-cell (24 hphCG) or four-cell stages (60 hphCG) were collected in PBS, and the volume was adjusted to 10–15 μl in Laemmli's buffer, 5% β-mercaptoethanol. The samples were denatured by heating for 10 min at 95°C and subjected to 10% SDS–PAGE for 1.5 h at 18 mA. Separated proteins were transferred onto 0.2-μm nitrocellulose (Bio-Rad Laboratories, Hercules, CA) and were revealed as described (Zatsepina *et al.*, 2000), using either the anti-RPA116 polyclonal antibody (dilution 1:4000), the anti-UBF serum (dilution 1:5000), or the anti-fibrillarin serum (1:2000) and the appropriate horseradish peroxidase-conjugated secondary antibodies (Sigma; dilution 1:100,000). The signal was developed with the Pierce West DURA detection system (Perbio Sciences, Bezons, France). For controls, total NIH3T3 cell extracts were prepared and probed under the same conditions.

RESULTS

Ribosomal DNA Transcription Is Activated in Two-Cell Embryos around 45 hphCG

To analyze in detail the building-up of a functional nucleolus, we ought to know as precisely as possible the time of the onset of rRNA synthesis. A very suitable and sensitive method for that is the microinjection of BrUTP, followed by its immunodetection with specific antibodies (Bouniol-Baly *et al.*, 1999).

None of the two-cell embryos microinjected with BrUTP in the presence of α-amanitin and fixed at 40 hphCG showed any sign of BrUTP incorporation, while in the same experiments, 97% of the embryos showed incorporation in the absence of α-amanitin, i.e., were active for pol II-dependent transcription (Table 1). These results confirm that pol II-dependent transcription was already restored by that time (Bouniol *et al.*, 1995). At 45 hphCG, an average of 37% of the embryos was able to incorporate BrUTP in the presence of α-amanitin; this proportion increased to 100% at 48.5 hphCG (Table 1).

At all time points, BrUTP signals were seen as discrete spots associated with the NPB surface or more extended threads emanating from NPBs to the nucleoplasm (Figs. 1A–1C). From analysis of *in toto* images combined with a series of confocal sections, it was clear that nascent transcripts were not associated with all NPBs, but with only 5–7 among the 12–15 present at that stage (Figs. 1A–1C, asterisk), even at the times where rDNA transcription was achieved in 100% of the 2-cell embryos. We also noted that the precursor microinjected to 1 blastomere at 45–48 hphCG could not diffuse to the second blastomere, which thus remained unlabeled. However, if the 2 blastomeres were microinjected, both of them incorporated BrUTP (n = 13, 45 hphCG). Thus, pol I-dependent transcription is activated simultaneously in the 2 blastomeres of 2-cell embryos.

TABLE 1

pol I- and pol II-Dependent Transcription Activities in Two-Cell Mouse Embryos As a Function of Time after hCG Injection

Time after hCG injection (h)	pol I + pol II activity (%)	pol I activity (%)
40	31/32 (97)	0/46 (0)
45	12/13 (92)	10/27 (37)
45.5	17/17 (100)	44/98 (45)
48.5	n.d.	18/18 (100)

Note. n.d., not determined.

Organization of the rRNA Synthesis and Processing Machineries in Transcriptionally Active Two-Cell Embryos

To analyze the organization of the pol I-dependent machinery when rRNA synthesis was turned on, we performed coimmunodetection of BrUTP and UBF. At 45 as well as 48 hphCG, UBF was detected in all pol I-active embryos, mostly in groups of small discrete foci aligned at the NPB periphery. All small UBF foci were associated with rDNA transcription sites, and usually occupied the center of BrUTP labeled areas "emanating" from them (Figs. 1A and 1B). In addition to these small foci, one or two larger UBF spots were seen, which were, however, not associated with transcription (Fig. 1C, arrow). While double immunolabeling for BrUTP and RPA116 could not be performed since both primary antibodies are mouse mAbs, double immunolabeling for RPA116 and UBF showed a complete coincidence of the two proteins within both the small foci and the large spots (Fig. 1D; also see Fig. 3C).

Then, we addressed the question of how the pre-rRNA processing machinery was organized in embryos where rDNA transcription was activated. In all transcriptionally active embryos analyzed at 45–48 hphCG, fibrillarin showed a complex distribution. It was found accumulated in: (1) one to three large roundish patch(es) located close (or associated with) NPBs, (2) small foci associated with the NPB surface, and (3) partial peri-NPB crescents (Fig. 2A). Serial confocal images showed that the "fibrillarin crescents" were, *per se*, composed of accumulations of fibrillarin-positive foci, arranged in "necklaces" (Fig. 2A). The fibrillarin-positive foci and crescents were associated with BrUTP-incorporation sites, whereas large fibrillarin patches were completely devoid of transcription signals,

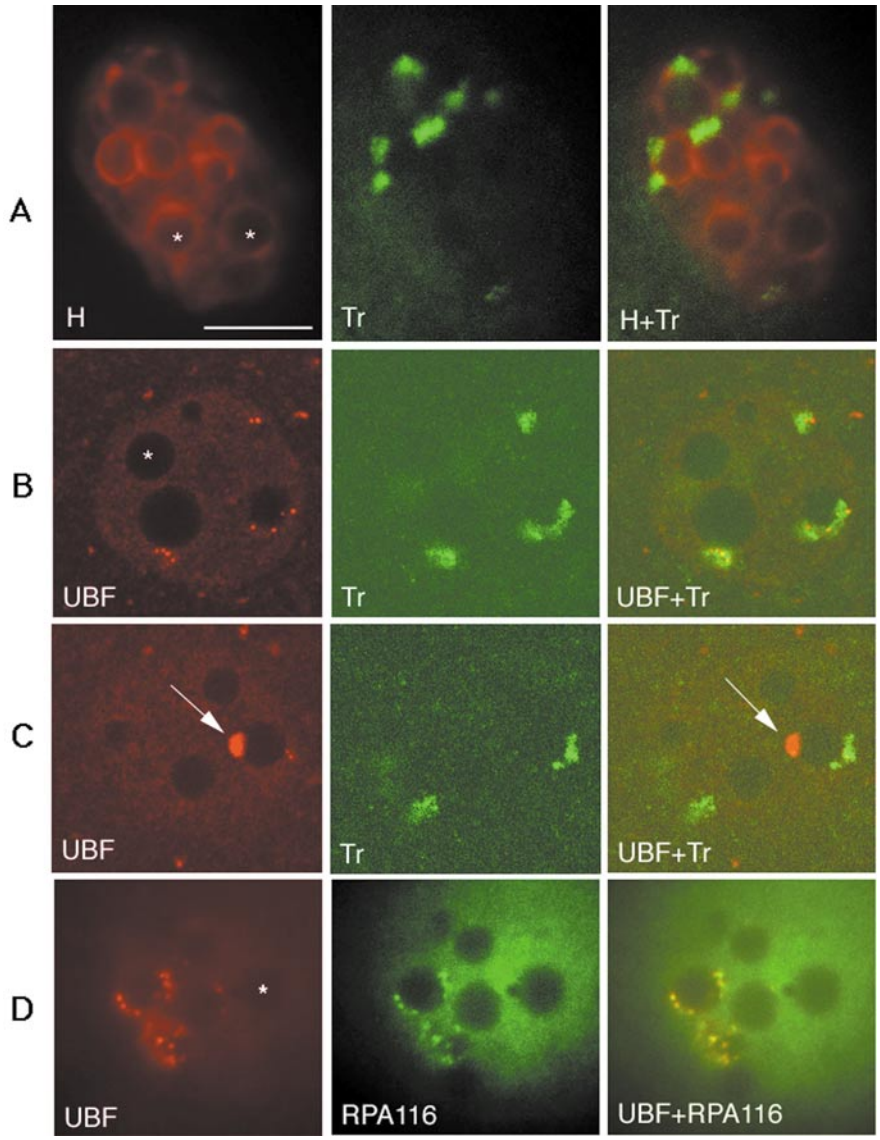

FIG. 1. Localization of the nascent rRNA transcripts and the pol I-dependent transcription machinery in active two-cell mouse embryos (48 hphCG). (A) Double labeling with Hoechst 33342 for DNA (H, in false *red* color) and BrUTP for the rRNAs (Tr, *green*). *Merged* image is shown in the right column (H+Tr). Two NPBs, which are excluded from rDNA transcription, are indicated by (*). Conventional microscopy. (B, C) Double immunolabeling for UBF (*red*) and rDNA transcription (Tr, *green*). Confocal microscopy images of two different optical planes through the same two-cell embryo. *Merged* images are in the right column (UBF+Tr). UBF foci are associated with the nascent rRNAs. One NPB (*) and one large UBF patche (*arrow*) are devoid of associated transcription. (D) Double immunolabeling for UBF (*red*) and RPA116 (*green*). *Merged* image in the right column (UBF + 116) shows the complete colocalization of the two signals. One NPB (*) is excluded from rDNA transcription. Conventional microscopy. All images taken with a 100× objective. Bar, 10 μm

although they could be associated with a NPB involved in rDNA transcription (Figs. 2B and 2C, arrows). Coimmunostaining for fibrillarin and B23, a protein involved in late rRNA processing and preribosome assembly, showed that B23 accumulated around the fibrillarin/BrUTP-positive areas, but was entirely excluded from the large fibrillarin-rich patches (Fig. 2D). Noteworthy, the NPBs, which were not associated with fibrillarin/BrUTP, were also devoid of B23 (Fig. 2D, asterisk).

Coimmunostaining for UBF and fibrillarin could not be performed, as both antigens were recognized by autoimmune human sera. However, coimmunolabeling of two-cell embryos for RPA116 and fibrillarin showed that fibrillarin labeling was always coincident with RPA116 labeling,

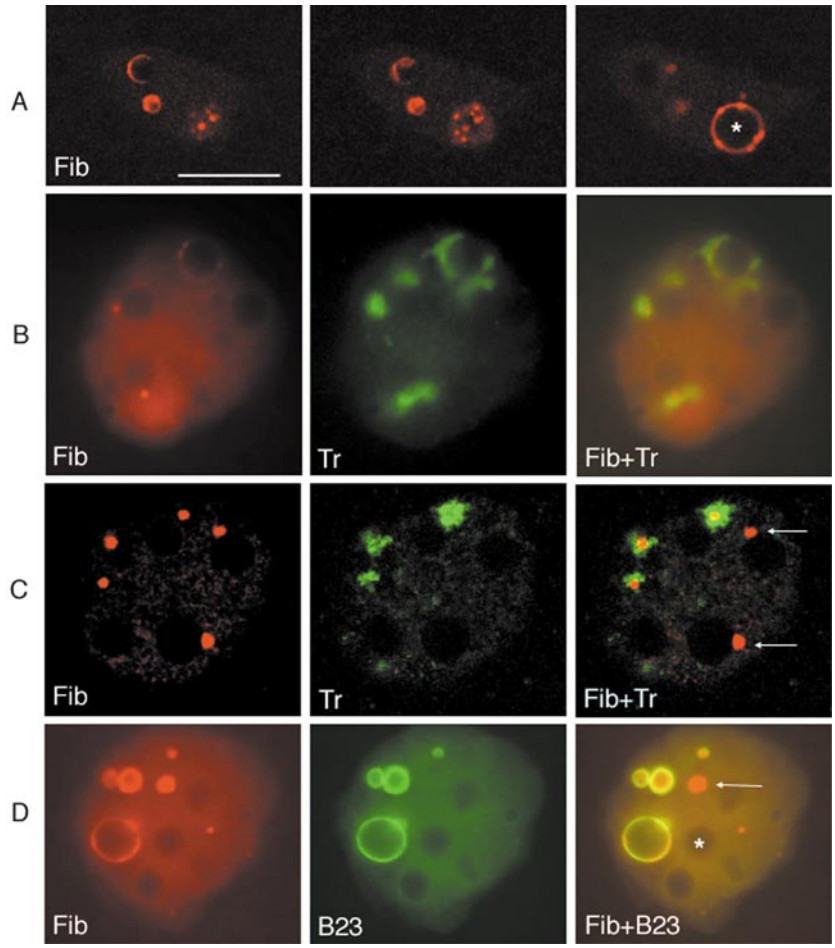

FIG. 2. Distribution of fibrillarin (Fib), B23 (B23), and rDNA transcription sites (Tr) in transcriptionally active two-cell embryos. (A) At 48 hphCG, three consecutive confocal sections (Z-step = 0.8 μm) of a nucleus of a two-cell embryo labeled for fibrillarin. Note the accumulation of fibrillarin foci at the upper and medium part of the NLB marked with an asterisk (*). (B, C) At 45 hphCG, double immunolabeling for fibrillarin (Fib, *red*) and rRNA transcripts (Tr, *green*) viewed by conventional (B) or confocal (C) microscopy. Fibrillarin foci are at the center of nascent rRNA signals, except for two large patches (C, *arrows*) which are devoid of associated transcription signals. (D) At 48h phCG, double immunolabeling for fibrillarin (Fib, *red*) and B23 (*green*). Good colocalization of the two proteins is seen. A large fibrillarin patch (*arrow*) is not labeled for B23. A NPB negatively stained for fibrillarin and B23 is indicated by (*). Conventional microscopy. All images taken with a 100× objective. Bar, 10 μm

although it covered larger areas (data not shown). Thus, in embryos active in pol I-dependent transcription, the pol I transcription and rRNA processing factors accumulate in discrete regions at the periphery of a limited number of NPBs, whereas other NPBs are devoid of any associated transcripts and proteins.

The pol I Transcription Machinery Is Reassembled before Activation of rDNA Transcription

As mentioned above, activation of rDNA transcription was first detected in middle/late two-cell embryos. However, we noticed that transcriptionally silent embryos fixed at 40 hphCG could be positively labeled for UBF and RPA116. These observations prompted us to analyze the dynamics of the major proteins of the pol I-transcription machinery during the period preceding the onset of transcription.

UBF and RPA116 were not detected at the one-cell stage and not earlier than 37 hphCG at the two-cell stage (Fig. 3A). At 37 hphCG, the two proteins were detected individually in a small proportion of embryos (UBF in 7/35 and RPA116 in 4/29 embryos, respectively; see Table 2). They were accumulated in one or two large spots close to, or even at the surface of, a NPB (Fig. 3B). Starting from 40 hphCG, in addition to the above described large spots, groups of smaller foci were observed at the periphery of some NPBs (Fig. 3C), as in nuclei active in pol I-dependent transcription (see above). Table 2 summarizes the evolution of UBF and RPA116 labeling in two-cell embryos as a function of time

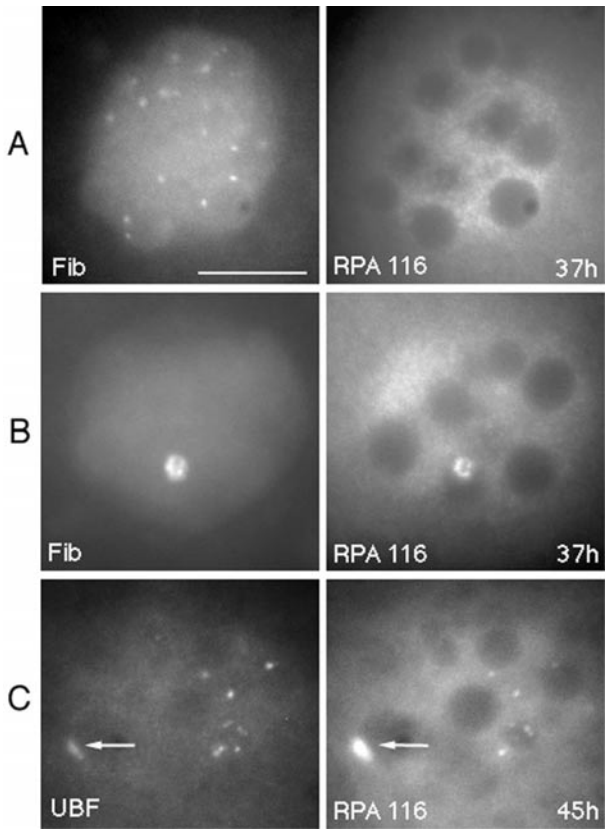

FIG. 3. Relative distribution of RPA116, UBF, and fibrillarin (Fib) in nuclei of two-cell embryos at different stages of the cell cycle. (A) At 37 hphCG, fibrillarin is distributed in small foci, while RPA116 is not detected. (B) At 37 hphCG, in some embryos, RPA116 is accumulated within a large patch where it coincides with fibrillarin. (C) At 45 hphCG, UBF and RPA116 are colocalized, in both the large patch (*arrows*) and small foci. Conventional microscopy with a 100× objective. Bar, 10 μm

after hCG injection. It shows that (1) the proportion of UBF/RPA116-positive embryos increases progressively, and (2) among them, the proportion of two-cell embryos with small peri-NPB foci increases also, but with a certain lag-time. Data from Table 2 also suggest that small peri-NPB spots appear later for RPA116 than for UBF. This discrepancy is, however, only apparent and most probably due to the asynchrony of embryos among the various experiments, including single and double labeling, which are summarized in Table 2. Indeed, in all experiments where coimmunostaining for UBF and RPA116 was performed, a perfect colocalization of the two proteins was observed (Fig. 3C).

The analysis of UBF pattern as a function of the rDNA transcriptional activity (Table 3) showed that none of the nuclei presenting only one big spot were active in pol I-dependent transcription, while small peri-NPB UBF spots could be found in embryos with undetectable levels of pol I-dependent transcription. Finally, in the vast majority of cases, nuclei of the two blastomeres had the same UBF pattern.

In order to confirm that UBF accumulation, first in large patches, then in small peri-NPB foci, was not linked to a low level of pol I-dependent transcription which would not have been detected, two-cell embryos isolated either at 40 or 41.5 hphCG were cultured *in vitro* with 0.1 μg/ml or 0.25 μg/ml actinomycin D, respectively, until 45.5 hphCG, and then processed for UBF labeling. Neither the proportion of UBF-positive embryos (22/23 without actinomycin D vs 47/50 with actinomycin D) nor the distribution in large spots only, or large spots and small foci, was affected as compared with the untreated embryos.

TABLE 3

Patterns of UBF Labeling in Transcriptionally Active and Inactive Two-Cell Mouse Embryos (45 hphCG)

	UBF		
Transcriptional status of embryos	No labeling	One to three big patches only	One big patch + numerous small foci
Pol I-active	0/9 (0%)	0/9 (0%)	9/9 (100%)
Pol I-inactive	6/19 (31%)	6/19 (31%)	7/19 (38%)

TABLE 2

Patterns of Immunolabeling of Two-Cell Embryos for UBF and RPA116 at Various Time Points after hCG Injection

Time after hCG injection (no. of expt.)	UBF			RPA116		
	No labeling	One to three big patches only	One big patch + numerous small foci	No labeling	One to three big patches only	One big patch + numerous small foci
30–32 h (1 expt.)	6/6	0/6	0/6	6/6	0/6	0/6
37 h (3 expt.)	17/32 (80%)	7/35 (20%)	0/35	25/29 (86%)	4/29 (14%)	0/29
39/40 h (3 expt.)	24/59 (41%)	17/59 (29%)	18/59 (30%)	15/26 (58%)	11/26 (42%)	0/26
45 h (4 expt.)	11/80 (14%)	21/80 (26%)	48/80 (60%)	1/16 (6%)	3/16 (19%)	12/16 (75%)
48 h (2 expt.)	0/20	0/20	20/20	0/14	0/14	14/14
50/52 h (1 expt.)	0/22	0/22	22/22	0/22	0/22	22/22

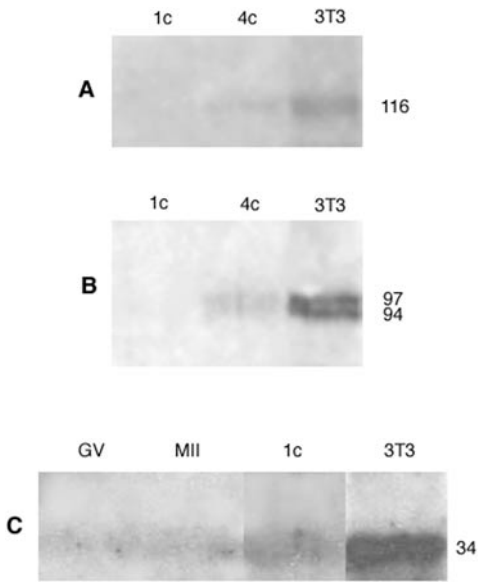

FIG. 4. Western blot detection of RPA116 (A), UBF (B), and fibrillarin (C) in mouse oocytes, one-cell, and four-cell embryos. (A, B) Extracts from 1.2×10^4 NIH3T3 cells (3T3), 200 embryos at the one-cell stage (1c), or 180 embryos at the four-cell stage (4c) were separated by 8% SDS–PAGE, transferred to nitrocellulose, and probed with anti-RPA116 (A) or anti-UBF (B) antibody. (C) Extracts from 3×10^4 NIH3T3 cells (3T3), 250 mouse oocytes at GV stage (GV), 190 oocytes at MII stage (MII), and 350 one-cell embryos (1-cell) were separated by 10% SDS–PAGE, transferred to nitrocellulose and probed with anti-fibrillarin antibody.

Previously, we showed that UBF and RPA116 are massively degraded in MII oocytes, as compared with the GV stage (Zatsepina *et al.*, 2000). We thus addressed the question of whether the progressive nuclear accumulation of UBF and RPA116 in the two-cell nuclei revealed by immunolabeling resulted from *de novo* synthesis of the two proteins. For this, we performed Western blots of total cell lysates prepared from one-cell (24 hphCG) and four-cell (60 hphCG) embryos. Figure 4 shows that the two proteins remain undetectable in transcriptionally silent one-cell embryos but are well detected in four-cell embryos where rRNA synthesis is active. These data indicate that negative labeling for UBF/RPA116 observed in one- and early two-cell embryos before activation of rDNA transcription was indeed due to the absence, or very low abundance, of the proteins, and was not due to retention in the cytoplasm or masking of the epitopes.

Fibrillarin Is Maternally Inherited and Organized in Specialized Subnuclear Domains from the One-Cell Stage Onwards

Contrary to UBF and RPA116, fibrillarin and B23 were both detected in early two-cell embryos, as soon as nuclei are formed (Table 2). In addition, previously published data showed that fibrillarin could be detected in one-cell embryos, where it was colocalized with coilin (Ferreira *et al.*, 1995). This prompted us to analyze in more detail the dynamics of fibrillarin and B23 during the first and second cell cycles relative to the distribution of coilin.

At the one-cell stage, fibrillarin could be detected neither in anaphase nor telophase female chromosomes ($n = 5$; not shown), nor over the decondensing sperm chromatin ($n = 7$; not shown). First detectable in both male and female pronuclei at the time of their formation (17–18 hphCG; Adenot *et al.*, 1991), fibrillarin was concentrated in numerous small bright foci associated with NPBs, which were also labeled for coilin (Fig. 5; 18 h, $n = 5$). Later on, between 19 and 28 hphCG, the number of NPB decreased (Debey *et al.*, 1989), and fibrillarin/coilin foci were reduced in number and more heterogenous in size. However, they remained associated with all NPBs (19 h, $n = 16$; 24 h, $n = 15$; 28 h, $n = 27$) (Fig. 5, 25 h). When chromatin started to condense in both pronuclei, as viewed by Hoechst 33242 staining, fibrillarin, but not coilin, accumulated transitorily within NPBs remnants (Fig. 5, 28 h, $n = 4$). Fibrillarin and coilin then became uniformly distributed in the cytoplasm upon completion of the mitotic chromosomes condensation. As far as B23 is concerned, it was found diffusely distributed in pronuclei of all ages (not shown). Chromosomes of the first cleavage mitosis were not labeled for any nucleolar protein studied (RPA116 and UBF, $n = 4$; fibrillarin and B23, $n = 10$).

To examine whether fibrillarin was at least in part maternally inherited, we analyzed parthenogenetically activated eggs. Irrespective of the way of egg activation (i.e., with ethanol or cycloheximide), the distribution of fibrillarin in parthogenetic embryos was similar to that in fertilized zygotes ($n = 13$; not shown). In line with these results, incubation of fertilized one-cell embryos with 50 μg/ml cycloheximide from 17 hphCG until 21 ($n = 7$) or 26 hphCG ($n = 7$), did not prevent immunolabeling of embryos for fibrillarin (not shown). Moreover, Western blots showed that, in MII oocytes and one-cell embryos, fibrillarin was present at a comparable level (Fig. 4C). Altogether, these data indicate that, in contrast to UBF and RPA116, a pool of fibrillarin is present in the oocyte cytoplasm, and fibrillarin regroupment around NPBs does not require the *de novo* synthesis of the protein.

Fibrillarin and Coilin Undergo a Complex Time-Dependent Rearrangement during the Two-Cell Stage

At early two-cell stage (30 hphCG), the distribution of fibrillarin and coilin was very similar to what it was at early one-cell stage, namely colocalization of the two proteins in numerous small foci located around all NPBs (Fig. 5, 30 h; and Fig. 6, pattern A). The distribution of the two proteins, however, was not completely coincident, as shown by the

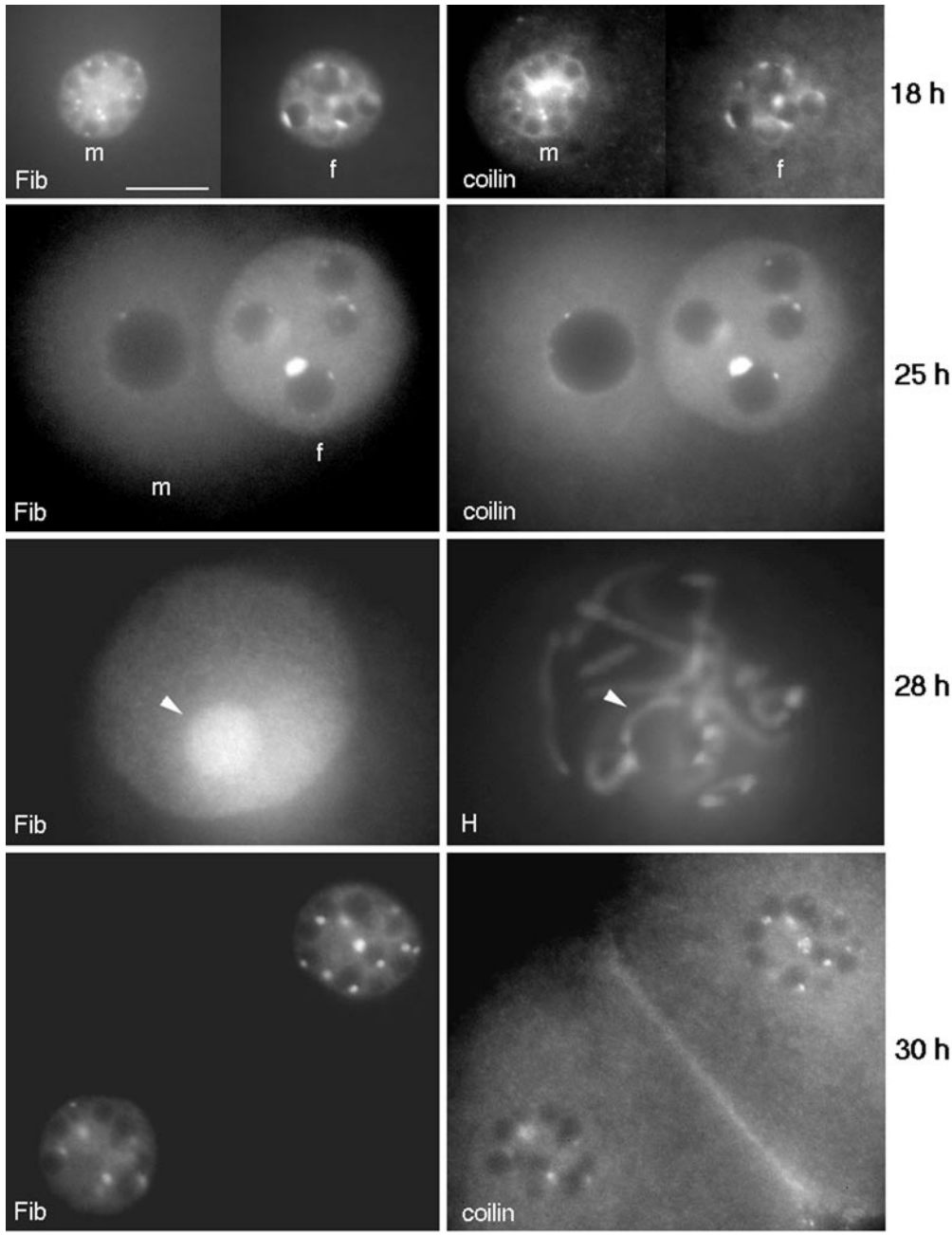

FIG. 5. Double immunolabeling for fibrillarin (Fib) and coilin (coilin) during the one-cell stage (from 18 to 28 hphCG) and at the beginning of the two-cell stage (30 hphCG). Fibrillarin and coilin are present in the male (m) and female (f) pronuclei as soon as they are formed (18 h). The two proteins are colocalized in small foci located at the periphery of all NPBs. These foci become more heterogeneous in size at 25 hphCG. At 28 hphCG, upon chromosome condensation (H, Hoechst 33342 staining), fibrillarin labels the interior of the NPB remnant (*arrowhead*). Fibrillarin and coilin are both present in small foci at the periphery of NPBs in two-cell nuclei from the beginning of their formation onwards (30 hphCG). Conventional microscopy with a 100× objective. Bar, 10 μm

distribution of the *red* and *green* signals (Fig. 6, arrowheads). B23, in contrast, was diffusely distributed (not shown).

Starting at 36–37 hphCG, the distribution of all three proteins underwent a profound reorganization leading to the appearance of different labeling patterns: (1) pattern B: small peri-NPB fibrillarin/coilin foci were less intense while a large patch heavily labeled with fibrillarin and coilin appeared (Fig. 6, pattern B). This body was generally

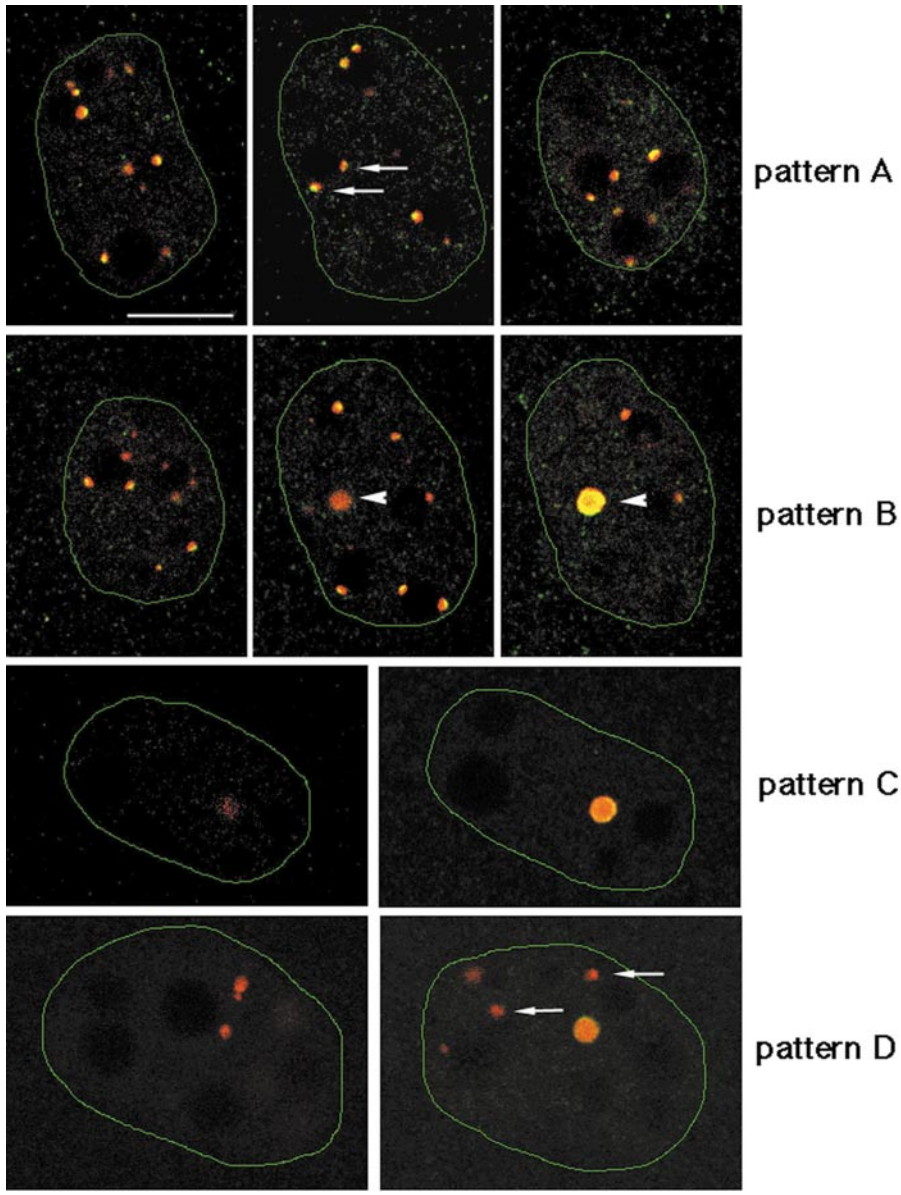

FIG. 6. Four patterns of fibrillarin (*red*) and coilin (*green*) distribution observed in two-cell nuclei between 37 and 45 hphCG. Each row represents a series of confocal images of a single nucleus obtained with a 100× objective and a 0.8-μm Z-step. **Pattern A**: Numerous small foci containing fibrillarin and coilin are seen around all NPBs. Sections 7, 12, and 20 are shown from the left to the right. Note that the two signals do not completely overlap in different foci (*arrows*), thus indicating unequal distribution of the two proteins. 37 hphCG. **Pattern B**: In addition to small foci, a large patch heavily labeled for fibrillarin and coilin is seen (*arrowheads*). Section numbers 10, 15, and 17 (from left to right). 37 hphCG. **Pattern C**: Small foci disappear, and only one big patch is present. Section numbers 3 and 6 (from left to right). 40 hphCG. **Pattern D**: Both fibrillarin and coilin are concentrated in a single large patch. In addition, fibrillarin is seen in small foci at the periphery of some NPBs, which are devoid of coilin (*arrows*). Section numbers 1 and 7 (from left to right). 45 hphCG. Bar, 10 μm

seen as a "cap" closely opposed to one NPB. This pattern was the most frequent at 37 hphCG (see Table 4). (2) Pattern C: the small peri-NPBs foci had disappeared, and only the large fibrillarin/coilin body, about 1 μm in diameter, was seen (Fig. 6, pattern C). This pattern was the most frequent at 40 hphCG (Table 4). In embryos exhibiting patterns B and C, B23 remained diffusely distributed (Fig. 7A). (3) Pattern D: in addition to the large coilin-containing body, fibrillarin was again found in small foci, first spatially separated, then organized as necklaces or crescent-like structures around

TABLE 4
Immunocytochemical Location of fibrillarin, B23, and coilin as a Function of Time in Two-Cell Embryos

Time after hCG injection (no. of expt.)	fibrillarin			B23		coilin	
	Small foci around all NPBs	A large patch with or without a few small foci	A large patch + small foci or crescents	Uniform	NPB-associated	Small foci around all NPBs	Only one to three large patches
30–32 h (1 expt.)	6/6	0/6	0/6				
37 h (2 expt.)	17/32 (53%)	11/32 (47%)	0/32	4/4	0/4		
39–40 h (3 expt.)	7/26 (27%)	12/26 (46%)	7/26 (27%)	3/6 (50%)	3/6 (50%)	0/9	9/9
41 h (1 expt.)						0/11	11/11
45 h (2 expt.)	1/30 (3%)	19/30 (63%)	10/30 (33%)	2/7 (28.5%)	5/7 (71.5%)	1/21 (5%)	20/21 (95%)
46 h (1 expt.)	2/18 (11%)	7/18 (39%)	9/18 (50%)				
48–48.5 h (4 expt.)	0/52	5/52 (12.5%)	47/52 (90%)			0/29	29/29
50 h (1 expt.)			10/10		5/5		
52 h (1 expt.)			12/12		12/12		

some NPBs, as described above (Fig. 2). Coilin was completely absent from these peri-NPB fibrillarin-positive foci and crescents (Fig. 6, pattern D, arrow). The reverse was true for B23, which was absent from the large body (Fig. 7C) but accumulated around the same NPBs, which were labeled with fibrillarin (see Fig. 2D). This pattern was found in 100% of 48-hphCG-old embryos (Table 4). Note again that this regroupment left many NPBs devoid of any association with fibrillarin, coilin or B23, thus indicating their unequal implication in the assembly of nucleolar factors.

In summary, contrary to UBF and RPA116, fibrillarin and B23 were present from the beginning of the two-cell stage and showed a complex two phases dynamics: the first phase, from cleavage to 37–40 hphCG led to the progressive regroupment of fibrillarin and coilin from small peri-NPB foci toward a single (or 2/3) large body, while B23 remained diffusely distributed; the second, starting at 37–40 hphCG, led to the appearance of new types of fibrillarin foci at the periphery of some NPBs, devoid of coilin but associated with B23. Thus, at any given time, the distribution of the different labeling patterns reflects the respective speed of these two processes (Table 4).

Large Fibrillarin/Coilin Bodies Share Common Features with Cajal Bodies and Recruit pol I-Dependent Transcription Machinery

To further characterize the large nuclear body that accumulated coilin and fibrillarin, we performed double immunolabeling of one- and two-cell embryos with the polyclonal anti-coilin antibody and the monoclonal antibody Y12, which recognizes the Sm proteins, a set of protein characteristic of the snRNPs involved in RNA splicing (Will *et al.*, 1993). These proteins are known to be markers of the CBs. Y12 labeled both the small coilin foci present in one-cell and early two-cell embryos (not shown) and the periphery of the large coilin-containing nuclear body present in middle and late two-cell embryos (Fig. 7D, arrow). In addition, YI2 also accumulates in intranuclear domains corresponding to the interchromatin granules ("speckles") previously shown to be present at the two-cell stage (Vautier *et al.*, 1994). Altogether, these findings indicate that the small fibrillarin foci present in early two-cell embryos and the large coilin-containing nuclear body present in middle and late two-cell embryos harbor the Sm proteins. They can thus be considered as pCBs and true CBs, respectively.

The regroupment of fibrillarin and coilin in a single large CB at the middle of two-cell stage (37–40 hphCG) corresponds to the time when UBF and RPA116 labeling first appeared. We thus decided to analyze whether there was a correlation between these two processes. Double immunostaining for coilin and RPA116, coilin and UBF, or fibrillarin and RPA116 in 37-hphCG-old embryos showed that, when first detected, RPA116 and UBF were indeed accumulated in the CBs (Fig. 7B)

Starting from the End of the Four-Cell Stage, Active pol I Transcription and Processing Machineries Are Functionally Organized at the NPB Surface

At mitosis, eight to nine UBF spots or doublets (one per chromatid) were associated with chromosomes, most probably attached to NORs (n = 24; Fig. 8A). When mitosis occurred in blastomeres which had been previously microinjected with BrUTP in the presence of α-ammanitin, BrUTP labeling could be seen around UBF spots (Fig. 8B). This signal could represent nascent transcripts close to the NORs but not really attached to them or transcripts in the process of being elongated and still bound to the rDNA [transcripts containing modified nucleotides may not be properly processed (Wansink *et al.*, 1993)]. Chromosomes, however, were never labeled for RPA116 (n = 33; data not shown), B23 (n = 9; data not shown), or fibrillarin (n = 14; Fig. 8C).

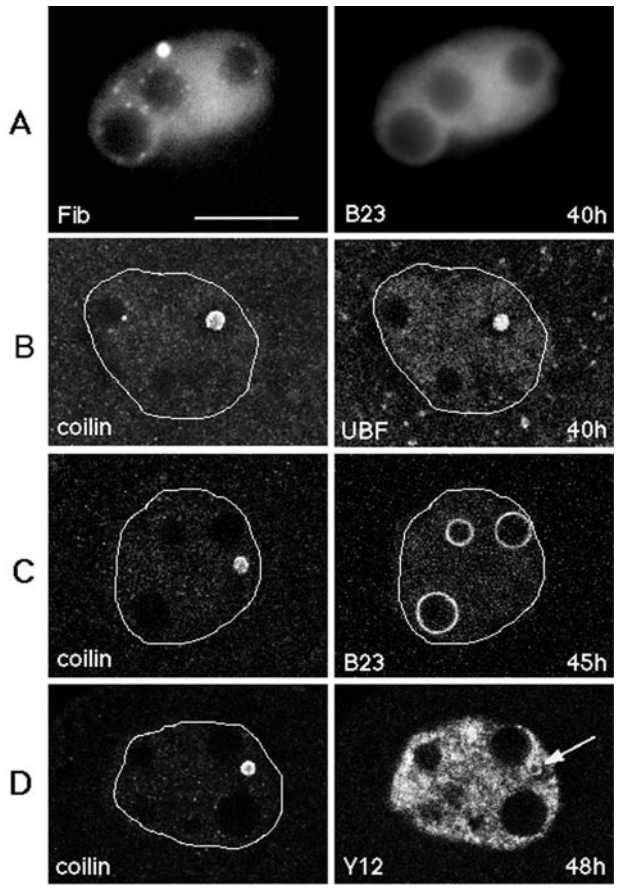

FIG. 7. Relative distribution of fibrillarin (Fib), B23, UBF, coilin, and Sm proteins (Y12) at the different stages of the two-cell cycle. (A) At 40 hphCG, in nuclei exhibiting the pattern B-type of fibrillarin labeling (Fig. 6), B23 is uniformly distributed within the nucleoplasm. Conventional microscopy with a 100× objective. (B) At 40 hphCG, when UBF labeling is first detected, it is associated with a large patch also labeled for coilin. (C) At 45 hphCG, B23 accumulates around some NPBs, but is excluded from the patch labeled for coilin. (D) At 48 hphCG, the large coilin-containing patch is also labeled at its periphery by Y12 mAb (*arrow*). (B–D) Confocal microscopy images obtained with a 100× objective. Bar, 10 μm

At the 4-cell stage, the proteins studied seemed to follow a very similar dynamics as those at the 2-cell stage, namely first appearance of fibrillarin/coilin foci (pCBs) at the periphery of NPBs (Figs. 9A and 9A′), followed by the emergence of 1–3 larger CBs, and the migration of fibrillarin, but not coilin around 4–6 of the 8–10 NPBs present at that stage leaving the other unlabeled (Figs. 9B and 9B′). B23 formed a continuous intense rim around the same NPBs (Figs. 9D and 9D′). RPA116 and UBF were colocalized in a series of discrete spots around the fibrillarin/B23-positive NPBs (Figs. 9C and 9C′). At the middle of the 4-cell stage (60 hphCG), the number of NPBs was reduced to 3–6 of heterogenous size. They were all surrounded by a large zone labeled for fibrillarin/B23 (Figs. 9F and 9F′) and numerous radial fibrils labeled for UBF/RPA116 (Figs. 9E and 9E′). This labeling pattern was consistent with the presence of a reticulated network of compartments resembling the FC and DFC observed at the ultrastructural level at the periphery of NPBs at that stage (Geuskens and Alexandre, 1984; Takeuchi and Takeuchi, 1986).

At the third mitosis (4- to 8-cell transition), chromosomal NORs were again labeled for UBF (8–9 spots or doublets, $n = 4$), but neither for RPA116 ($n = 4$) nor for fibrillarin or B23 ($n = 8$, data not shown). Starting from the 8-cell stage onwards, the number of NPBs was reduced to 2–4, all associated with both transcription and processing machineries (Figs. 9G–9H′), thus indicating that they could be considered as true functional nucleoli. The high number of UBF and RPA116 foci associated with each NPB supported the idea of a high rRNA synthesis activity. Starting from the fourth division (8- to 16-cell division), chromosomes were labeled for both UBF and RPA116 ($n = 2$; Fig. 8E) and were decorated with fibrillarin ($n = 3$; Fig. 8D).

DISCUSSION

Recent data have greatly advanced the understanding of the nucleolar reassembly after mitosis and during *Xenopus laevis* development (Fomproix *et al.*, 1998; Dundr *et al.*, 1997, 2000; Verheggen *et al.*, 1998, 2000; Savino *et al.*, 2001; Dousset *et al.*, 2000). Development in mammals proceeds differently, however, than in *X. laevis*, with a succession of true cell cycles. Knowledge of the molecular mechanisms governing reactivation of ribosomal genes and reassembly of a functional nucleolus are completely missing in such systems. The present work addresses these problems and provides new insight into nucleologenesis in mouse preimplantatory development.

At first, it was necessary to know as precisely as possible the timing of the rRNA synthesis reactivation. By statistical analysis of more than 100 embryos microinjected with BrUTP/α-amanitin, we could show that nascent pre-rRNAs are first observed at the middle-end of the second cell cycle, around 44–45 hphCG, and simultaneously in the 2 blastomeres. Transcription sites are associated with the surface of NPBs, in agreement with previous data (Koberna *et al.*, 1998), and we showed here for the first time that they are also associated with small UBF/pol I (RPA116) foci, which decorate the NPBs as necklace-like structures, and thus represent ribosomal gene-bound transcription complexes. Furthermore, the major transcription factors are actually assembled at their rDNA targets at 40 hphCG, i.e., 4–5 h before the onset of rDNA transcription.

A mechanism which could regulate the pol I complex assembly is the availability of the endogenous factors. Indeed, we showed by Western blots that, in one-cell (rDNA transcriptionally silent) embryos, UBF and RPA116 remain at the low level characteristic for MII oocytes (Zatsepina *et*

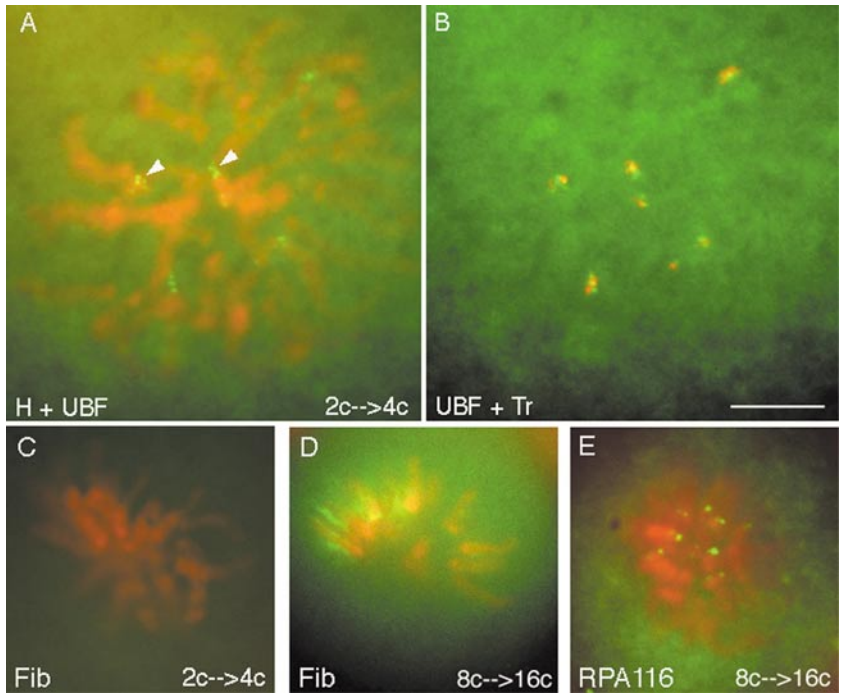

FIG. 8. Labeling of metaphase chromosomes during the second (2c→4c, A–C), and fourth (8c→16c, D, E) cleavage divisions for some nucleolar proteins. (A, B) Double labeling of the same embryo for DNA (H, shown in a false *red* color) and UBF (*green*) (in A), or UBF (*green*) and rRNA transcripts (Tr, *red*) (in B). UBF is seen within single or double (*arrowheads*) spots located over a few chromosomes and is associated with BrUTP-rRNAs. The embryo was squeezed between slides to spread the chromosomes. (C) Immunolabeling of chromosomes for fibrillarin is completely negative. Chromosomes are shown in a false *red* color. (D, E) Chromosomes are enwrapped by fibrillarin (D, *green*) and labeled for RPA116 (E, *green*). Chromosomes were stained with Hoechst 33342, but are shown in a false *red* color. Conventional light microscopy with a 100× objective. Bar, 10 μm.

al., 2000), whereas their abundance increases at the four-cell stage, when ribosomal genes are actively transcribed. Similar developmental changes were previously described in preimplantation mouse embryos for the TATA box-binding protein (TBP) (Worrad *et al.*, 1994), which is also a partner of the rDNA transcription complex (Roussel *et al.*, 1996). Therefore, one could assume that endogenous expression of rDNA transcription factors is a prerequisite for the pol I complex assembly. Whether the maternally inherited mRNAs or newly formed mRNA transcripts are utilized for the translation of RPA116 and UBF proteins still remains an open question.

The timing of the reassembly of the pol I complex corresponds also to the end of the replication phase (Moore *et al.*, 1996). It is generally admitted that DNA replication is a period of facilitated access of transcription factors to their DNA-binding sequences, through displacement of nucleosomes and modulation of chromatin structure (Schultz *et al.*, 1999). Our present data would be in line with this idea.

rDNA transcription was not detected within the NPB core and is highly unlikely to occur there, due to the well-established absence of DNA (Flechon and Kopecny, 1998). Nevertheless, the NPB core seems to act as a "structural support" for the activation of rDNA transcription, but the underlying mechanisms are poorly understood, essentially because of the compactness of this body, which precludes any analysis of its content. In that respect, the labeling of NPB remnants with fibrillarin antibody during condensation of pronuclei at the end of the one-cell stage is remarkable (Fig. 5, 28 h). Experiments are underway to characterize the two-cell rDNA transcription domains at the ultrastructural level (Migné, unpublished observations). It must also be recalled that NPBs of similar size and ultrastructure can be obtained upon fusion of somatic cell nuclei with activated oocytes (Borsuk *et al.*, 1996), thus offering another situation to analyze the nature and role of the NPB core.

Most strikingly, we found that the population of NPBs is heterogenous in their ability to be associated with transcription factors and active transcription sites. There are usually 5–7 "active" (i.e., associated with rRNA synthesis) NPBs among the 12–15 present in 2-cell blastomere nuclei. One hypothesis is that active NPBs are in contact with several NOR-bearing chromosomes, while inactive NPBs may contact chromosomes not bearing NORs or bearing

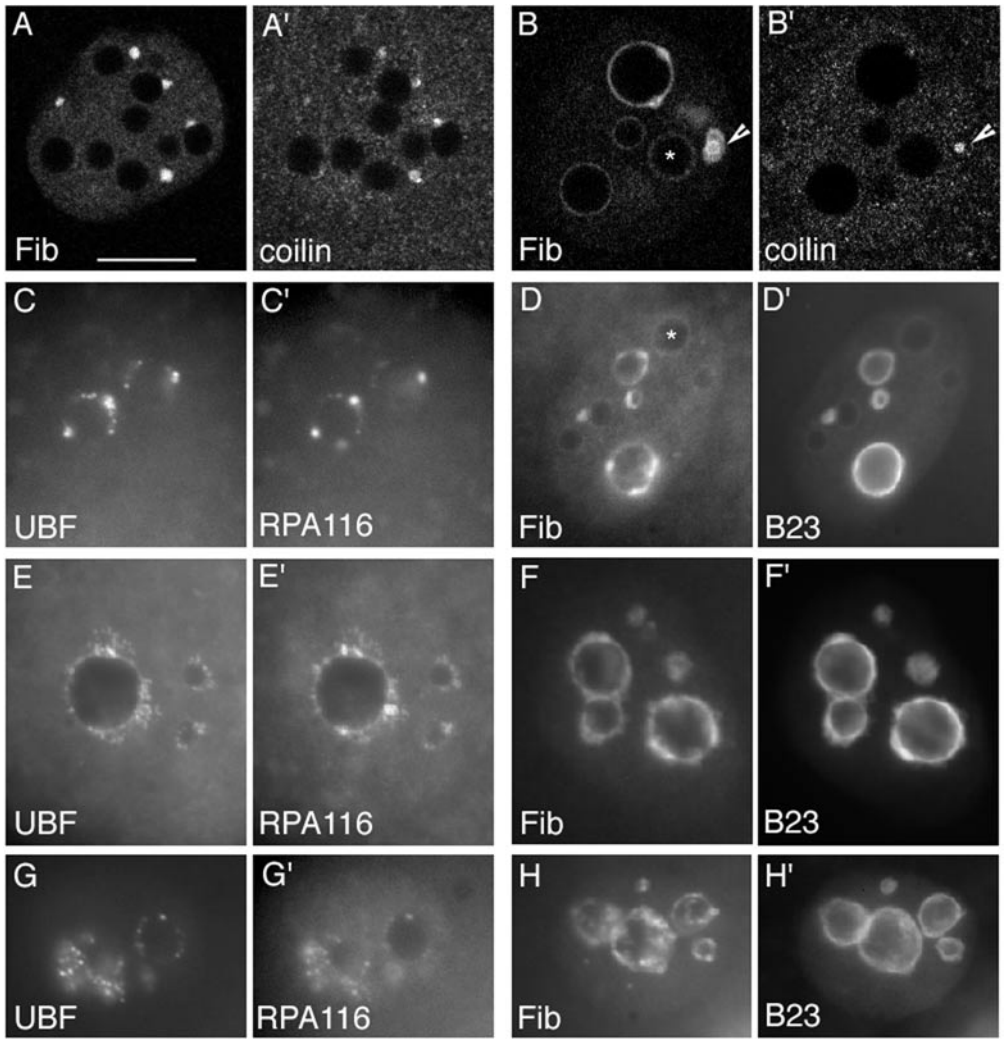

FIG. 9. Distribution of the major nucleolar proteins and coilin in four- and eight-cell embryos. (A, A′) At 49 hphCG, shortly after formation of the four-cell nuclei, fibrillarin (Fib) and coilin are colocalized in small foci at the periphery of NPBs. (B, B′ and D, D′) At 50 hphCG, fibrillarin is concentrated in a large patch (Cajal body) also labeled for coilin (B′, *arrowhead*) and forms an irregular layer around some NPBs also labeled for B23 (D′). The Cajal body is associated to two NPBs in the process of fusion (B, *arrowhead*). *Asterisks* indicate NPBs, which are not associated with fibrillarin and B23. (C, C′) At 50 hphCG, UBF and RPA116 are colocalized in the foci associated with the periphery of some NPBs. (E, E′ and F, F′) At 60 hphCG, UBF/RPA116 foci (E, E′) form necklace-like structures emanating from NPBs. Fibrillarin and B23 (F, F′) are concentrated in large zones surrounding the NPBs. Note that all NPBs are labeled, despite the fact that they are very heterogenous in size. (G, G′ and H, H′) UBF/RPA116 (G, G′) and fibrillarin/B23 (H, H′) labeling of eight-cell embryos. Note numerous UBF/RPA116 foci located at the periphery of NPBs. (A, A′, and B, B′) are by confocal, the others by conventional microscopy; images taken with a 100× objective Bar, 10 μm.

inactive NORs (see below). Another, nonmutually exclusive, possibility is that all NPB do not have the same composition and only some of them are able to recruit pol I transcription factors.

Most interestingly, before appearing in the transcription sites, rDNA transcription factors are first recruited to a large nuclear body that also contains fibrillarin, coilin, and the Sm proteins, and can thus be considered as CBs (Ferreira and Carmo-Fonseca, 1995). This is to our knowledge the first demonstration, in mammalian cells, of the recruitment of pol I and UBF in the CBs. In *Xenopus* oocytes, pol I, pol II, and pol III were located by immunofluorescence in CBs, together with various factors required for the transcription and processing of all classes of RNA (Gall *et al.*, 1999). In addition, two subunits of pol II, RPB6 and RPB9, were targeted to CBs rapidly after their translation (Morgan *et al.*, 2000). This led to the hypothesis that CBs could be the sites of preassembly of the transcription and processing

complexes (transcriptosomes) (Gall *et al.,* 1999; Gall, 2000, 2001). Our present results fit perfectly with this hypothesis, in a the situation of *de novo* synthesis of pol I and UBF (see above). It remains nevertheless to be determined whether (1) Pol I and UBF accumulation in CBs is a necessary step in their assembly and targeting to NPBs, and (2) the population of proteins located in CBs serves as "reservoir" for the active complexes or represents a different stable population. Note that Nopp140, another protein belonging to both the nucleolus and the CB (Isaac *et al.,* 1998), follows in mouse embryos the same labeling pattern as fibrillatin (Baran *et al.,* 2001), in agreement with the idea of a functional link between the two compartments.

Actually, the formation of the CB is preceded by the appearance of smaller pCBs at the surface of NPBs. The collection of images obtained on two-cell embryos suggests that large CBs do not result from the coalescence of small pCB, but rather from the transfer of both coilin and fibrillarin from the pCB to the CB, similar to the migration of material between different postmitotic PNBs (Savino *et al.,* 2001). Also, fibrillarin and coilin seem to be inequally distributed in all pCBs, probably reflecting an intense trafficking of the proteins among the various nuclear compartments (Platani *et al.,* 2000). Interestingly, unlike the situation with respect to the rDNA transcription machinery, all NPBs are equivalent in their ability to recruit coilin.

Subsequent to, or just concomitant with, the formation of the CB and prior to any ongoing rDNA transcription, part of the fibrillarin pool is redistributed, together with B23, around the active NPB. A similar situation was observed in *X. laevis* development (Verheggen *et al.,* 1998, 2000). However, we could not detect here any equivalent of the PNBs described in the later system as well as in somatic cells after mitosis (Ochs *et al.,* 1985a; Jimenez-Garcia *et al.,* 1994; Verheggen *et al.,* 1998, 2000). Nucleologenesis in mouse embryos thus seems to proceed through the direct recruitment of processing factors to the NORs, as recently described to occur in somatic cells early in telophase before the fusion of prepackaged PNBs (Dousset *et al.,* 2000). In the latter case, pre-rRNAs were shown to be involved in the recruitment process (Dousset *et al.,* 2000). The possible presence of pre-rRNA of maternal origin was not studied here, but it is worth recalling that NPBs of early embryos have been shown to contain RNA, some of it synthesized in the latest stages of oocyte growth (Biggiogera *et al.,* 1994; Kopecny *et al.,* 1995).

It has long been known that in mouse embryos the so called "Ag-NOR proteins," which are characteristic for active ribosomal genes, associate with the chromosomal NORs starting from the second cleavage mitosis (Dyban *et al.,* 1990; Engel *et al.,* 1977). The complete set of the NOR-associated proteins during somatic mitosis is still not completely known, but a few of them were identified, namely pol I (RPA190), UBF, p135, p50, TBP, and a TBP-associated factor, TAF_I100 (Roussel *et al.,* 1996).

Noteworthy, we found here that the number of chromosomes harboring UBF during the successive mitoses is close to the expected number in the mouse, 10 (Henderson *et al.,* 1976), and does not vary, which suggests that all NORs are active. In contrast, the set of proteins associated with chromosomal NOR varies with the cleavage division considered: UBF is associated with chromosomal NORs as soon as after the onset of rDNA transcription (second cleavage), whereas NOR-bound RPA116 and perichromosomal fibrillarin were only detected starting from the fourth cleavage mitosis (Fig. 8). One could speculate that the lack of stable association of the pol I/UBF complex to mitotic chromosomes at the first three cleavages is caused by (1) an "immature status" of the pol I transcription initiation complex that might lack some auxiliary factors, (2) a too low abundance of the corresponding proteins, or yet (3) a perturbed regulation of rRNA processing.

At any rate, the mitotic behavior of the major nucleolar proteins seems to be restored at the fourth mitotic cleavage. This argues in favor of the idea that, at the preceding cell cycle (i.e., 8-cell), the faithful rDNA transcription and rRNA processing are completely restored.

ACKNOWLEDGMENTS

We thank Dr. I. Grummt for the anti-RPA116 antibody, Dr. R. Ochs for the mouse anti-fibrillarin mAb, Dr. P. K. Chan for the mouse mAb anti-B23 antibody, Dr. A. Lamond for the anti-coilin antibody, and Dr. J. A. Steiz for the anti-Sm Y12 mAb. This work was supported by funds from the Institut National de la Recherche Agronomique (INRA), from the Muséum National d'Histoire Naturelle (MNHN), and from INTAS (Grant 96-1638). Confocal microscopy was performed in the IFR 63 facilities. We are grateful to Mr. M. Bomakodo for animal care.

REFERENCES

Adenot, P. G., Szollosi, M. S., Geze, M., Renard, J. P., and Debey, P. (1991). Dynamics of paternal chromatin changes in live one-cell mouse embryo after natural fertilization. *Mol. Reprod. Dev.* **28,** 23–34.

Aoki, F., Worrad, D. M., and Schultz, R. M. (1997). Regulation of transcriptional activity during the first and second cell cycles in the preimplantation mouse embryo. *Dev. Biol.* **181,** 296–307.

Azum-Gelade, M. C., Noaillac-Depeyre, J., Caizergues-Ferrer, M., and Gas, N. (1994). Cell cycle redistribution of U3 snRNA and fibrillarin. Presence in the cytoplasmic nucleolus remnant and in the prenucleolar bodies at telophase. *J. Cell Sci.* **107,** 463–475.

Baran, V., Brochard, V., Renard, J. P., and Fléchon, J. E. (2001). Nopp 140 involvement in nucleologenesis of mouse preimplantation embryos. *Mol. Reprod. Dev.* **59,** 277–284.

Baran, V., Vesela, J., Rehak, P., Koppel, J., and Fléchon, J. E. (1995). Localization of fibrillarin and nucleolin in nucleoli of mouse preimplantation embryos. *Mol. Reprod. Dev.* **40,** 305–310.

Biggiogera, M., Burki, K., Kaufmann, S. H., Shaper, J. H., Gas, N., Amalric, F., and Fakan, S. (1990). Nucleolar distribution of proteins B23 and nucleolin in mouse preimplantation embryos as visualized by immunoelectron microscopy. *Development* **110,** 1263–1270.

Biggiogera, M., Malatesta, M., Abolhassani-Dadras, S., Amalric, F., Rothblum, L. I., and Fakan, S. (2001). Revealing the unseen: The organizer region of the nucleolus. *J. Cell Sci.* **114,** 3199–3205.

Biggiogera, M., Martin, T. E., Gordon, J., Amalric, F., and Fakan, S. (1994). Physiologically inactive nucleoli contain nucleoplasmic ribonucleoproteins: Immunoelectron microscopy of mouse spermatids and early embryos. *Exp. Cell Res.* **213,** 55–63.

Bohmann, K., Ferreira, J. A., and Lamond, A. I. (1995). Mutational analysis of p80 coilin indicates a functional interaction between coiled bodies and the nucleolus. *J. Cell Biol.* **131,** 817–831.

Borsuk, E., Szollosi, M. S., Besomebes, D., and Debey, P. (1996). Fusion with activated mouse oocytes modulates the transcriptional activity of introduced somatic cell nuclei. *Exp. Cell Res.* **225,** 93–101.

Bouniol, C., Nguyen, E., and Debey, P. (1995). Endogenous transcription occurs at the 1-cell stage in the mouse embryo. *Exp. Cell Res.* **218,** 57–62.

Bouniol-Baly, C., Hamraoui, L., Guibert, J., Beaujean, N., Szollosi, M. S., and Debey, P. (1999). Differential transcriptional activity associated with chromatin configuration in fully grown mouse germinal vesicle oocytes. *Biol. Reprod.* **60,** 580–587.

Carmo-Fonseca, M., Pepperkok, R., Carvalho, M. T., and Lamond, A. I. (1992). Transcription-dependent colocalization of the U1, U2, U4/U6, and U5 snRNPs in coiled bodies. *J. Cell Biol.* **117,** 1–14.

Clegg, K. B., and Piko, L. (1983). Quantitative aspects of RNA synthesis and polyadenylation in 1-cell and 2-cell mouse embryos. *J. Embryol. Exp.* **74,** 169–182.

Cmarko, D., Verschure, P. J., Rothblum, L. I., Hernandez-Verdun, D., Amalric, F., van Driel, R., and Fakan, S. (2000). Ultrastructural analysis of nucleolar transcription in cells microinjected with 5-bromo-UTP. *Histochem. Cell Biol.* **113,** 181–187.

Cuadros-Fernandez, J. M., and Esponda, P. (1996). Immunocytochemical localisation of the nucleolar protein fibrillarin and RNA polymerase I during mouse early embryogenesis. *Zygote* **4,** 49–58.

Debey, P., Renard, J. P., Coppey-Moisan, M., Monnot, I., and Geze, M. (1989). Dynamics of chromatin changes in live one-cell mouse embryos: A continuous follow-up by fluorescence microscopy. *Exp. Cell Res.* **183,** 413–433.

Derenzini, M., Thiry, M., and Goessens, G. (1990). Ultrastructural cytochemistry of the mammalian cell nucleolus. *J. Histochem. Cytochem.* **38,** 1237–1256.

Dousset, T., Wang, C., Verheggen, C., Chen, D., Hernandez-Verdun, D., and Huang, S. (2000). Initiation of nucleolar assembly is independent of RNA polymerase I transcription. *Mol. Biol. Cell* **11,** 2705–2717.

Dundr, M., Meier, U. T., Lewis, N., Rekosh, D., Hammarskjold, M. L., and Olson, M. O. (1997). A class of nonribosomal nucleolar components is located in chromosome periphery and in nucleolus-derived foci during anaphase and telophase. *Chromosoma* **105,** 407–417.

Dundr, M., and Misteli, T. (2001). Functional architecture in the cell nucleus. *Biochem. J.* **356,** 297–310.

Dundr, M., Misteli, T., and Olson, M. O. (2000). The dynamics of postmitotic reassembly of the nucleolus. *J. Cell Biol.* **150,** 433–446.

Dundr, M., and Raska, I. (1993). Nonisotopic ultrastructural mapping of transcription sites within the nucleolus. *Exp. Cell Res.* **208,** 275–281.

Dyban, A. P., Severova, E. L., Zatsepina, O. V., and Chentsov, Y. S. (1990). The silver-stained NOR and argentophilic nuclear proteins in early mouse embryogenesis: A cytological study. *Cell Differ. Dev.* **29,** 165–179.

Engel, W., Zenzes, M. T., and Schmid, M. (1977). Activation of mouse ribosomal RNA genes at the 2-cell stage. *Hum. Genet.* **38,** 57–63.

Fakan, S., and Odartchenko, N. (1980). Ultrastructural organization of the cell nucleus in erarly mouse embryos. *Biol. Cell* **37,** 211–218.

Ferreira, J., and Carmo-Fonseca, M. (1995). The biogenesis of the coiled body during early mouse development. *Development* **121,** 601–612.

Flechon, J. E., and Kopecny, V. (1998). The nature of the "nucleolus precursor body" in early preimplantation embryos: A review of fine-structure cytochemical, immunocytochemical and autoradiographic data related to nucleolar function. *Zygote* **6,** 183–191.

Fomproix, N., Gebrane-Younes, J., and Hernandez-Verdun, D. (1998). Effects of anti-fibrillarin antibodies on building of functional nucleoli at the end of mitosis. *J. Cell Sci.* **111,** 359–372.

Fomproix, N., and Hernandez-Verdun, D. (1999). Effects of anti-PM-Scl 100 (Rrp6p exonuclease) antibodies on prenucleolar body dynamics at the end of mitosis. *Exp. Cell Res.* **251,** 452–464.

Fulton, B. P., and Whittingham, D. G. (1978). Activation of mammalian oocytes by intracellular injection of calcium. *Nature* **273,** 149–151.

Gall, J. G. (2000). Cajal bodies: The first 100 years. *Annu. Rev. Cell Dev. Biol.* **16,** 273–300.

Gall, J. G. (2001). A role for cajal bodies in assembly of the nuclear transcription machinery. *FEBS Lett.* **498,** 164–167.

Gall, J. G., Bellini, M., Wu, Z., and Murphy, C. (1999). Assembly of the nuclear transcription and processing machinery: Cajal bodies (coiled bodies) and transcriptosomes. *Mol. Biol. Cell* **10,** 4385–4402.

Gautier, T., Robert-Nicoud, M., Guilly, M. N., and Hernandez-Verdun, D. (1992). Relocation of nucleolar proteins around chromosomes at mitosis. A study by confocal laser scanning microscopy. *J. Cell Sci.* **102,** 729–737.

Gebrane-Younes, J., Fomproix, N., and Hernandez-Verdun, D. (1997). When rDNA transcription is arrested during mitosis, UBF is still associated with non-condensed rDNA. *J. Cell Sci.* **110,** 2429–2440.

Geuskens, M., and Alexandre, H. (1984). Ultrastructural and autoradiographic studies of nucleolar development and rDNA transcription in preimplantation mouse embryos. *Cell Differ.* **14,** 125–134.

Hadjiolov, A. A. (1985). The nucleolus and ribosome biogenesis. (M. Alfert, W. Beermann, L. Goldstein, K. R. Porter, and P. Sitte, Eds.), p. 268. Springer-Verlag, New York.

Henderson, A. S., Eicher, E. M., Yu, M. T., and Atwood, K. C. (1976). Variation in ribosomal RNA gene number in mouse chromosomes. *Cytogenet. Cell Genet.* **17,** 307–316.

Isaac, C., Yang, Y., and Meier, U. T. (1998). Nopp 140 functions as a molecular link between the nucleolus and the coiled bodies. *J. Cell Biol.* **27,** 319–329.

Jimenez-Garcia, L. F., Segura-Valdez, M. L., Ochs, R. L., Rothblum, L. I., Hannan, R., and Spector, D. L. (1994). Nucleologenesis: U3 snRNA-containing prenucleolar bodies move to sites of active pre-rRNA transcription after mitosis. *Mol. Biol. Cell* **5,** 955–966.

Kirschner, M., Newport, J., and Gerhart, J. (1985). The timing of early developmental events in Xenopus. *Trends Genet.* **1,** 41–47.

Knowland, J., and Graham, C. (1972). RNA synthesis at the two-cell stage of mouse development. *J. Embryol. Exp. Morphol.* **27,** 167–176.

Koberna, K., Landa, V., Kanka, J., Pliss, A., Eltsov, M., Stanek, D., and Raska, I. (1998). Non-isotopic detection of nucleolar transcription in pre-implantation mouse embryos. *Reprod. Nutr. Dev.* **38,** 117–126.

Kopecny, V., Biggiogera, M., Laurincik, J., Pivko, J., Grafenau, P., Martin, T. E., Fu, X. D., and Fakan, S. (1996). Fine structural cytochemical and immunocytochemical analysis of nucleic acids and ribonucleoprotein distribution in nuclei of pig oocytes and early preimplantation embryos. *Chromosoma* **104,** 561–574.

Kopecny, V., Landa, V., and Pavlok, A. (1995). Localization of nucleic acids in the nucleoli of oocytes and early embryos of mouse and hamster: An autoradiographic study. *Mol. Reprod. Dev.* **41,** 449–458.

Latham, K. E. (1999). Mechanisms and control of embryonic genome activation in mammalian embryos. *Int. Rev. Cytol.* **193,** 71–124.

Lyon, C. E., Bohmann, K., Sleeman, J., and Lamond, A. I. (1997). Inhibition of protein dephosphorylation results in the accumulation of splicing snRNPs and coiled bodies within the nucleolus. *Exp. Cell Res.* **230,** 84–93.

Magoulas, C., Zatsepina, O. V., Jordan, P. W., Jordan, E. G., and Fried, M. (1998). The SURF-6 protein is a component of the nucleolar matrix and has a high binding capacity for nucleic acids in vitro. *Eur. J. Cell Biol.* **75,** 174–183.

Moore, G. D., Ayabe, T., Kopf, G. S., and Schultz, R. M. (1996). Temporal patterns of gene expression of G1-S cyclins and cdks during the first and second mitotic cell cycles in mouse embryos. *Mol. Reprod. Dev.* **45,** 264–275.

Morgan, G. T., Doyle, O., Murphy, C., and Gall, J. G. (2000). RNA polymerase II in cajal bodies of amphibian oocytes. *J. Struct. Biol.* **129,** 258–268.

Narayanan, a., Speckmann, W., Terns, R., and Terns, M. P. (1999). Role of the box C/D motif in localization of small nucleolar RNAs to coiled bodies and nucleoli. *Mol. Biol. Cell* **10,** 2131–2147.

Nothias, J. Y., Miranda, M., and DePamphilis, M. L. (1996). Uncoupling of transcription and translation during zygotic gene activation in the mouse. *EMBO J.* **15,** 5715–5725.

Ochs, R. L., Lischwe, M. A., Shen, E., Carroll, R. E., and Busch, H. (1985a). Nucleologenesis: Composition and fate of prenucleolar bodies. *Chromosoma* **92,** 330–336.

Ochs, R. L., Lischwe, M. A., Spohn, W. H., and Busch, H. (1985b). Fibrillarin: A new protein of the nucleolus identified by autoimmune sera. *Biol. Cell* **54,** 123–133.

Ochs, R. L., and Press, R. I. (1992). Centromere autoantigens are associated with the nucleolus. *Exp. Cell Res.* **200,** 339–350.

Olson, M. O., Dundr, M., and Szebeni, A. (2000). The nucleolus: An old factory with unexpected capabilities. *Trends Cell Biol.* **10,** 189–196.

Platani, M., Goldberg, I., Swedlow, J. R., and Lamond, A. I. (2000). In vivo analysis of Cajal body movement, separation, and joining in live human cells. *J. Cell Biol.* **151,** 1561–1574.

Prather, R., Simerly, C., Schatten, G., Pilch, D. R., Lobo, S. M., Marzluff, W. F., Dean, W. L., and Schultz, G. A. (1990). U3 snRNPs and nucleolar development during oocyte maturation, fertilization and early embryogenesis in the mouse: U3 snRNA and snRNPs are not regulated coordinate with other snRNAs and snRNPs. *Dev. Biol.* **138,** 247–255.

Raska, I., Andrade, L. E., Ochs, R. L., Chan, E. K., Chang, C. M., Roos, G., and Tan, E. M. (1991). Immunological and ultrastructural studies of the nuclear coiled body with autoimmune antibodies. *Exp. Cell Res.* **195,** 27–37.

Roussel, P., Andre, C., Comai, L., and Hernandez-Verdun, D. (1996). The rDNA transcription machinery is assembled during mitosis in active NORs and absent in inactive NORs. *J. Cell Biol.* **133,** 235–246.

Roussel, P., Andre, C., Masson, C., Geraud, G., and Hernandez-Verdun, D. (1993). Localization of the RNA polymerase I transcription factor hUBF during the cell cycle. *J. Cell Sci.* **104,** 327–337.

Savino, T. M., Gebrane-Younes, J., De Mey, J., Sibarita, J. B., and Hernandez-Verdun, D. (2001). Nucleolar assembly of the rRNA processing machinery in living cells. *J. Cell Biol.* **153,** 1097–1110.

Scheer, U., and Hock, R. (1999). Structure and function of the nucleolus. *Curr. Opin. Cell Biol.* **11,** 385–390.

Scheer, U., and Rose, K. M. (1984). Localization of RNA polymerase I in interphase cells and mitotic chromosomes by light and electron microscopic immunocytochemistry. *Proc. Natl. Acad. Sci. USA* **81,** 1431–1435.

Schultz, R. M., Davis, W., Jr., Stein, P., and Svoboda, P. (1999). Reprogramming of gene expression during preimplantation development. *J. Exp. Zool.* **285,** 276–282.

Shaw, P. J., and Jordan, E. G. (1995). The nucleolus. *Annu. Rev. Cell Dev. Biol.* **11,** 93–121.

Sleeman, J., Lyon, C. E., Platani, M., Kreivi, J. P., and Lamond, A. I. (1998). Dynamic interactions between splicing snRNPs, coiled bodies and nucleoli revealed using snRNP protein fusions to the green fluorescent protein. *Exp. Cell Res.* **243,** 290–304.

Sleeman, J. E., and Lamond, A. I. (1999). Newly assembled snRNPs associate with coiled bodies before speckles, suggesting a nuclear snRNP maturation pathway. *Curr. Biol.* **9,** 1065–1074.

Spector, D. L., Ochs, R. L., and Busch, H. (1984). Silver staining immunofluorescence and immunoelectron microscopic localization of nucleolar phosphoproteins B23 and C23. *Chromosoma* **90,** 139–148.

Takeuchi, I. K., and Takeuchi, Y. K. (1986). Ultrastructural localization of Ag-NOR proteins in full-grown oocytes and preimplantation embryos of mice. *J. Electron Microsc. (Tokyo)* **35,** 280–287.

Thiry, M., Cheutin, T., O'Donohue, M. F., Kaplan, H., and Ploton, D. (2000). Dynamics and three-dimensional localization of ribosomal RNA within the nucleolus. *RNA* **6,** 1750–1761.

Thiry, M., and Goessens, G. (1991). Distinguishing the sites of pre-rRNA synthesis and accumulation in Ehrlich tumor cell nucleoli. *J. Cell Sci.* **99,** 759–767.

Thompson, E. M., Legouy, E., Christians, E., and Renard, J. P. (1995). Progressive maturation of chromatin structure regulates HSP70.1 gene expression in the preimplantation mouse embryo. *Development* **121,** 3425–3437.

Vautier, D., Besombes, D., Chassoux, D., Aubry, F., and Debey, P. (1994). Redistribution of nuclear antigens linked to cell proliferation and RNA processing in mouse oocytes and early embryos. *Mol. Reprod. Dev.* **38,** 119–130.

Verheggen, C., Almouzni, G., and Hernandez-Verdun, D. (2000). The ribosomal RNA processing machinery is recruited to the nucleolar domain before RNA polymerase I during *Xenopus laevis* development. *J. Cell Biol.* **149,** 293–306.

Verheggen, C., Le Panse, S., Almouzni, G., and Hernandez-Verdun, D. (1998). Presence of pre-rRNAs before activation of polymerase I transcription in the building process of nucleoli during early development of *Xenopus laevis*. *J. Cell Biol.* **142,** 1167–1180.

Voit, R., Hoffmann, M., and Grummt, I. (1999). Phosphorylation by G1-specific cdk-cyclin complexes activates the nucleolar transcription factor UBF. *EMBO J.* **18,** 1891–1899.

Wansink, D. G., Schul, W., van der Kraan, I., van Steensel, B., van Driel, R., and de Jong, L. (1993). Fluorescent labeling of nascent RNA reveals transcription by RNA polymerase II in domains scattered throughout the nucleus. *J. Cell Biol.* **122,** 283–293.

Whitten, W. K. (1971). Nutrien requirements for the culture of preimplantation embryos in vitro. *Adv. Biosci.* **6,** 129–139.

Will, C. L., Behrens, S. E., and Luhrmann, R. (1993). Protein composition of mammalian spliceosomal snRNPs. *Mol. Biol. Reprod.* **18,** 121–126.

Worrad, D. M., Ram, P. T., and Schultz, R. M. (1994). Regulation of gene expression in the mouse oocyte and early preimplantation embryo: Developmental changes in Sp1 and TATA box-binding protein, TBP. *Development* **120,** 2347–2357.

Zatsepina, O. V., Bouniol-Baly, C., and Amirand, C. (2000). Functional and molecular reorganization of the nucleolar apparatus in maturing mouse oocytes. *Dev. Biol.* **223,** 354–370.

Zatsepina, O. V., Todorov, I. T., Philipova, R. N., Krachmarov, C. P., Trendelenburg, M. F., and Jordan, E. G. (1997). Cell cycle-dependent translocations of a major nucleolar phosphoprotein, B23, and some characteristics of its variants. *Eur. J. Cell Biol.* **73,** 58–70.

Zatsepina, O. V., Voit, R., Grummt, I., Spring, H., Semenov, M. V., and Trendelenburg, M. F. (1993). The RNA polymerase I-specific transcription initiation factor UBF is associated with transcriptionally active and inactive ribosomal genes. *Chromosoma* **102,** 599–611.

Received for publication August 29, 2002
Revised September 30, 2002
Accepted October 1, 2002
Published online November 20, 2002